

# ASCA Observation of the Nearest Gravitational Lensing Cluster Candidate – A 3408

Haruyoshi KATAYAMA, Kiyoshi HAYASHIDA, and Kiyoshi HASHIMOTODANI

*Graduated School of Osaka University, 1-1, Machikaneyama, Toyonaka, Osaka 560-0043*

*hkatayam@ess.sci.osaka-u.ac.jp*

(Received 2001 February 23; accepted 2001 September 28)

## Abstract

We observed the nearest gravitational lensing cluster candidate, A 3408 ( $z = 0.042$ ), with ASCA. The projected mass profile of A 3408 was determined from the ICM temperature and the  $\beta$ -model parameters obtained with ASCA, assuming that the hot gas is spherically symmetric and in hydrostatic equilibrium. The projected mass within an arc radius,  $r_{\text{arc}}$ , of 110 kpc is  $M(r_{\text{arc}}) = 1.2_{-0.4}^{+0.8} \times 10^{13} M_{\odot}$ . This is 18 – 45% of the mass previously derived from a lensing analysis by Campusano et al. (1998, AAA 069.160.189) without any X-ray information.

The primary cause of this discrepancy is in their assumption that the center of the cluster potential coincides with the position of the brightest cluster galaxy (BCG), while we reveal the BCG position to be  $60''$  outside of the X-ray center. We further calculated a model for the source galaxy position and the gravitational potential that can reproduce both the X-ray data and the arc image. In this model, the magnification factor of the lens for the source galaxy was evaluated to be  $\Delta m = 0.07 \pm 0.03$  mag; i.e., the source galaxy is slightly magnified by the lens cluster A 3408.

**Key words:** galaxies: clusters: individual (A 3408) — X-rays: galaxies: clusters — X-rays: individual (A 3408)

## 1. Introduction

Clusters of galaxies are the largest gravitationally bound systems in the universe, which set clear constraints on the formation of the structure and composition of the universe. Furthermore, the gravitational mass of clusters is an important observational quantity to constrain the density parameter,  $\Omega$ .

There are primarily two methods to estimate the total (gravitational) mass of clusters of galaxies. One method employs X-ray observations under the assumption of hydrostatic equilibrium of the hot gas. The other uses the configuration of gravitational lensing arcs seen in optical observations. However, the mass estimates from lensing observations have been found to be systematically about 2-times larger than the mass estimates from X-ray observations (Wu, Fung 1997). Several ideas have been proposed to solve this discrepancy, including the following: (1) uncertainty in selecting the cluster center (Allen 1998; Hashimoto-dani 1999); (2) effect of the cooling flow (Allen 1998); and (3) mass profiles different from the conventional  $\beta$  model, e.g., the NFW density profile (Navarro et al. 1996).

In order to examine these possibilities, detailed X-ray observations of the central region of clusters are important. Such observations may be realized either with higher resolution instruments or equivalently by taking low- $z$  gravitational lensing clusters as targets. This is our motivation to observe low- $z$  gravitational lensing clusters.

Recently, several groups have found gravitational lensing clusters with low- $z$ . For instance, Allen, Fabian, and Kneib (1996) discovered a  $z = 0.43$  lensed arc in the massive cooling flow cluster PKS 0745–191 at  $z = 0.103$ . Blakeslee and Metzger (1999) discovered a lensed arc at  $z = 0.573$  in the nearby cD cluster A 2124 at  $z = 0.066$ . However, the lensing properties of these low- $z$  gravitational lensing clusters remain unclear. Especially, detailed X-ray observations of low- $z$  gravitational lensing clusters have rarely been performed. A 3408 at  $z = 0.042$  is the lowest- $z$  gravitational lensing cluster candidate in which arclike objects are found. In this paper, we present the results of an X-ray observation of A 3408 with ASCA.

For our study, we adopt  $\Omega_0 = 1$ ,  $\lambda = 0$ , and  $H_0 = 50h_{50}^{-1} \text{ km s}^{-1} \text{ Mpc}^{-1}$ ;  $1'$  corresponds to  $68 h_{50}^{-1} \text{ kpc}$  at the distance of the cluster.

## 2. Discovery of an Arc-like Object in A 3408

Because A 3408 has a relatively low galactic latitude ( $b = -17.57^\circ$ ), detailed optical observations have not been performed. According to the ACO catalog (Abell et al. 1989), the number of galaxies is 43 and the richness class is 0. Campusano and Hardy (1996) discovered an arc-like object near the center of A 3408. Figure 1 displays the  $B + I$  band image of A 3408. An arc-like object is  $\sim 50''$  away from the brightest cluster galaxy (BCG). The length of the arc-like object is  $\sim 11''$ , but its width is unresolved. The central elliptical galaxy has a redshift of 0.042, and the arc-like object has a redshift of 0.073. If the arc-like object is the lensed image of a background galaxy, A 3408 is the nearest gravitational lensing cluster that has been observed.

## 3. Lens Models of A 3408

Campusano et al. (1998) considered two lensing mass models to evaluate the projected mass within the arc radius, regarding the BCG as the center of the potential of A 3408.

*The minimum mass case (The BCG model):*

The mass distribution follows the light profile of the central brightest elliptical galaxy. The cluster component was not taken into account. The mass enclosed within  $r_{\text{arc}}$  (from the BCG to the arc) is  $M(r_{\text{arc}}) \sim 1.5 \times 10^{12} M_\odot$ , and the amplification of the source galaxy is  $\Delta m = 0.01$ .

*The maximum mass case (The dark-halo model):*

A typical massive dark-halo of cluster scale is assumed. They adopted a massive mass profile comparable to that found in A 2218. The mass enclosed within  $r_{\text{arc}}$  is  $M(r_{\text{arc}}) \sim 4.4 \times 10^{13} M_\odot$ , and the amplification of the source galaxy is  $\Delta m = 0.60$ .

Note that these models are based almost solely on a single arc image and that no X-ray information was employed. They could not determine which model is appropriate for the arc-like object.

## 4. ASCA Observations of A 3408

We observed A 3408 on 1999 March 13–14 with ASCA (Tanaka et al. 1994). With the exception of the ROSAT all-sky survey, no other X-ray observations had been carried out for this cluster. The

data from the Gas Imaging Spectrometer (GIS; Ohashi et al. 1996; Makishima et al. 1996) were taken in the PH mode, while those of the Solid-state Imaging Spectrometer (SIS) were acquired in the 2 CCD Faint mode. Because the SIS spectrum was severely distorted, possibly by a dark current, and its field of view is smaller than that of the GIS, we concentrated on the GIS data in a following analysis. The data selection was done using the standard screening parameters. We excluded the GIS data with a cutoff rigidity lower than 6 GV and those with elevation angles below  $5^\circ$  from the night-earth rim and  $25^\circ$  from the day-earth rim. After screening, the total exposure time was  $\simeq 50$  ks for the GIS.

Figure 2 shows the 0.7–10 keV GIS image of A 3408 (contour) overlaid on an optical image from the Digitalized Sky Survey (DSS). Extended emission from A 3408 is surely detected. The sky coordinates of the GIS image are adjusted to the point source, Seyfert 1 galaxy 1H0707–495, located at  $15'$  south to the center of the GIS field of view. It is found that the X-ray surface brightness peak of A 3408 is not coincident with the position of the BCG. The X-ray peak is  $\sim 60''$  away from the BCG (PGC 070830.4–491246). Considering a GIS pointing accuracy of  $24''$  (Gotthelf et al. 2000), we conclude that the BCG is not located at the X-ray peak, which we usually assume to be the center of the potential.

## 5. Spectral Analysis

We estimated the background spectrum by the following method. The non-X-ray background was reproduced with a method introduced by Ishisaki (1996). The cosmic X-ray background was extracted from the Large Sky Survey (Ueda et al. 1999) observed during the ASCA PV phase.

We fitted the GIS spectra with a single-temperature thermal-emission model by Raymond and Smith (1977). We fixed the hydrogen column density to the galactic absorption of  $N_{\text{H}} = 6.0 \times 10^{20} \text{ cm}^{-2}$  (Dickey, Lockman 1990) and the redshift to  $z = 0.042$ . We first extracted spectra from the region  $r < 250$  kpc and  $250 \text{ kpc} < r < 800$  kpc. The fit results are summarized in table 1.

The temperature of the region  $r < 250$  kpc is similar to that of the region  $250 \text{ kpc} < r < 800$  kpc. We also fitted the spectrum of the region within the arc radius ( $\sim 110$  kpc). The temperature of the region  $r < r_{\text{arc}}$  is  $3.0_{-0.3}^{+0.3}$  keV. These results imply a nearly isothermal nature for the ICM of A 3408.

We next extracted spectra from the combined region  $r < 800$  kpc. Figure 3 shows the spectrum of

the region  $r < 800$  kpc. The temperature of this region is  $2.9_{-0.2}^{+0.2}$  keV and the luminosity in the 2–10 keV energy band is  $L_X = 2.3_{-0.2}^{+0.1} \times 10^{43} h_{50}^{-2}$  erg s $^{-1}$ . The luminosity measured by the ROSAT all-sky survey in the 0.1–2.4 keV energy band is  $L_X = 5 \times 10^{43} h_{50}^{-2}$  erg s $^{-1}$  (Ebeling et al. 1996), which is consistent with our result derived from the spectral fitting ( $L_X = 4.5_{-0.1}^{+0.3} \times 10^{43} h_{50}^{-2}$  erg s $^{-1}$ ). The temperature of the ICM corresponds to a velocity dispersion of  $674_{-24}^{+22}$  km s $^{-1}$ , whereas we assume equal specific energy in the gas and galaxies.

## 6. Spatial Analysis

The X-ray surface brightness profile was extracted by accumulating photons within annular bins of  $0'.75$  width. We considered the X-ray peak as the center. Figure 4 shows the X-ray surface brightness profile of A 3408. We fitted the X-ray surface brightness profile with an isothermal  $\beta$  model. In the  $\beta$  model, the gas density profile is described as  $\rho_{\text{gas}}(r) = \rho_{\text{gas}0}/[1 + (r/r_c)^2]^{\frac{3\beta}{2}}$ , where  $\beta$  is the slope parameter of the outer part of the distribution and  $r_c$  is the core radius of the cluster. Assuming this density profile, the X-ray surface brightness profile is described as

$$S(b) = S_0 \frac{1}{\left(1 + \left(\frac{b}{r_c}\right)^2\right)^{3\beta-1/2}} + \text{background}, \quad (1)$$

where  $S_0$  is the central surface brightness and  $b$  is the projected 2D distance from the cluster center. Because of the complicated PSF of the ASCA XRT, we used a ray-tracing simulation (Ikebe et al. 1996) to fit the radial profile. The fit results are shown in figure 4 and table 2. The profile is well fitted with a single  $\beta$  model and doesn't exhibit a significant excess X-ray emission from the central region, which is expected for a cooling flow. Note that the core radius and  $\beta$  are similar to the typical value of nearby clusters determined by Einstein observations (Abramopoulos, Ku 1983).

We also fitted the same profile with an isothermal gas model in the NFW potential. The gas-density profile is analytically modeled as  $\rho_{\text{gas}}(r) = \rho_{\text{gas}0}/[1 + (r/r_s)]^{B\frac{r_s}{r}}$  (Makino et al. 1998). Here,  $r_s$  is the scaling parameter of the cluster, and  $B$  is the gradient of the gas density. The fit results are shown in figure 4 and table 3. There is little difference between two best-fit curves, and the  $\chi^2$  value of the NFW fit is similar to that of the  $\beta$  fit. Instruments with a better spatial resolution and a larger effective area

are needed to distinguish these models. In this paper, we adopt the  $\beta$ -model parameters to derive the mass distribution.

## 7. Mass Profile of A 3408

From the  $\beta$ -model parameters and the temperature of the ICM, we calculated the mass distribution of A 3408. Assuming hydrostatic equilibrium and neglecting the temperature gradient, the mass contained within a circle of radius  $b$  on the sky plane is given by

$$M(b) = 1.14 \times 10^{14} \beta \tilde{m}(b) \left(\frac{kT}{\text{keV}}\right) \left(\frac{r_c}{\text{Mpc}}\right) M_{\odot}, \quad (2)$$

where

$$\tilde{m}(b) = \frac{R_0^3}{1 + R_0^2} - \int_{b_0}^{R_0} x \sqrt{x^2 - b_0^2} \frac{3 + x^2}{(1 + x^2)^2} dx. \quad (3)$$

In equation (3),  $b_0 = b/r_c$  and  $R_0 = R/r_c$ , where  $R$  is the physical size of the cluster, for which we assumed 5 Mpc.

In order to estimate the uncertainty in our mass calculation, we employed the 90% confidence errors in the spectral and imaging parameters. Figure 5 shows the mass profile of A 3408 integrated along the line of sight. Each of the 27 lines corresponds to a combination of either the best-fit value or the 90% confidence lower or upper limit of the three parameters:  $\beta$ ,  $r_c$  and  $kT$ . The projected mass within the arc radius,  $r_{\text{arc}}$ , of 110 kpc is  $M(r_{\text{arc}}) = 1.2_{-0.4}^{+0.8} \times 10^{13} M_{\odot}$ .

We also applied polytropic models (Sarazin 1988) in which some temperature gradient in the intracluster gas is assumed. If the hot gas is strictly adiabatic, its pressure and density have a simple relation of  $P \propto \rho^{\gamma}$ . In this model,  $\gamma = 1$  implies that the gas distribution is isothermal. The hydrostatic mass contained within a sphere of a radius  $r$  is prescribed by

$$M(r) = -\frac{\gamma k T_{\text{gas}}(r)}{G \mu m_{\text{p}}} r \frac{d \ln \rho_{\text{gas}}}{d \ln r}, \quad (4)$$

where

$$T_{\text{gas}}(r) = T_{0,\gamma} \left(\frac{\rho_{\text{gas}}(r)}{\rho_0}\right)^{\gamma-1} = T_{0,\gamma} \left(1 + \frac{r^2}{r_c^2}\right)^{-3\beta(\gamma-1)/2}. \quad (5)$$

Markevitch et al. (1998) found universal temperature gradients in nearby rich clusters observed with ASCA, which are well described by the polytropic distribution with  $\gamma = 1.2 - 1.3$ , implying temperature increases toward the center. Therefore, we introduced a polytropic gas distribution with  $\gamma = 1.3$ . Although there is no observational evidence, we also tested the case with  $\gamma = 0.9$  for a temperature decrease toward the center. However, because the temperature gradient is significant in the region  $r > r_c$ , the range of the estimated mass is almost the same as that in the isothermal case,  $M(r_{\text{arc}}) = 1.2_{-0.4}^{+0.9} \times 10^{13} M_{\odot}$  ( $\gamma = 0.9$ ) and  $M(r_{\text{arc}}) = 1.4_{-0.5}^{+0.6} \times 10^{13} M_{\odot}$  ( $\gamma = 1.3$ ).

## 8. Discussion

### 8.1. Comparison with Models by Campusano et al.

The existence of hot gas extending over a few Mpc in A 3408 rejects the BCG model by Campusano et al. (1998), in which only the BCG was taken into account. The projected mass of A 3408 within the arc radius derived based on our X-ray observation is  $1.2_{-0.4}^{+0.8} \times 10^{13} M_{\odot}$ . This is 18 – 45% of the mass obtained from the dark-halo (cluster) model by Campusano et al. (1998). However, it should not be taken straightforward, since the center of the potential that they assumed, i.e., BCG, differs from the X-ray center that we defined. Furthermore, they assumed that the cluster mass profile of A 3408 is similar to that of a distant cluster, A 2218, while our mass profile is based on the X-ray observation of A 3408, itself. On these two points, we consider that our mass estimation based on the X-ray observation has some advantage over the mass estimation by Campusano et al. (1998).

Our mass model is based on the following assumptions: an isothermal gas distribution, hydrostatic equilibrium, and a spherically symmetric gas distribution. However, as mentioned in section 7, the range of the estimated mass is little affected by possible temperature gradients with  $\gamma = 1.3$  or 0.9. Meanwhile, if A 3408 is a merging or post-merging cluster, the assumptions of hydrostatic equilibrium and a spherically symmetric gas distribution would be inappropriate. However, the relatively regular X-ray surface-brightness distribution of A 3408 suggests that the cluster is a moderately relaxed system. This is also supported by the fact that the morphological classification of A 3408 is Bautz-Morgan Type I-II (Abell et al. 1989). In order to confirm that A 3408 is really a relaxed system, a further investigation,

such as concerning the velocity dispersion of member galaxies, is needed.

### 8.2. Potential Model Accounting for Both the X-ray Data and the Arc Image

For a given gravitational potential (cluster mass distribution) and a source position, the X-ray emission profile and the lensing arc image can be calculated. Conversely, we constrained the source position and the gravitational potential that reproduce the arc image and the X-ray data, as was done in Hattori et al. (1998) and in Hashimoto-dani (1999). We performed a similar analysis for A 3408. In addition to the potential of the cluster (we allow for deviations from spherical symmetry), the potential due to the BCG was considered, since, in several clusters of galaxies, bright galaxies near the arc are considered to play a significant role in lensing (Hattori et al. 1998, Hashimoto-dani 1999). The potential depth of the BCG was estimated by using the Faber–Jackson relation (Faber, Jackson 1976); it is  $\sim 300$  km s $^{-1}$  in terms of the velocity dispersion. Figure 6 shows the source position predicted by our model. The source position determined by Campusano et al. (1998) in their dark halo model is shown in the same figure as a reference. The magnification factor for the source galaxy is constrained to be  $\Delta m = 0.07 \pm 0.03$  mag. Thus, the source galaxy is only slightly magnified by the lens A 3408 in our potential model. The small magnification factor is also consistent with the slightly distorted image of the arc-like object.

Because of the small redshift of the source galaxy for the A 3408 lens, we have a good opportunity to study its intrinsic properties and the modification by the lens in detail. The characteristics of the source galaxy were discussed by Campusano et al. (1998) under the assumptions of their minimum mass case and the maximum mass case, for which they evaluated the source magnification factors to be  $\Delta m = 0.01$  and 0.60, respectively. On the other hand, we provided  $\Delta m = 0.07$ , which implies that the absolute magnitude,  $M_B$ , of the source galaxy is  $-18.7$ . According to the galaxy population statistics by Binggeli, Sandage, and Tammann (1988), about 75% of the field galaxies with the same absolute magnitude are spiral. Considering the small magnification factor,  $\Delta m = 0.07$ , of the lens, the source galaxy is not significantly modified in its shape, and should be regarded as an edge-on spiral originally. In this case, except for the small probability to realize an edge-on configuration, the low rotation velocity of the source galaxy measured by Campusano et al. (1998) might imply a somewhat extraordinary nature of the source

galaxy. This is because even the smallest Sc galaxies have twice the observed rotation velocity of the source galaxy, as mentioned by Campusano et al. (1998). Although further study is required concerning this point, this kind of examination is generally important for a nearby lensing object.

## 9. Summary

We observed the nearest gravitational lensing cluster candidate, A 3408, with ASCA. Our observation determined the ICM temperature and X-ray surface brightness profile of A 3408 for the first time. We also showed that the gas distribution of A 3408 is isothermal at the central region of A 3408, even within the arc radius.

We compared our mass model based on the X-ray observation with that of Campusano et al. (1998) based on the optical image. The mass derived by us is 18 – 45% of that by Campusano et al. (1998). The primary cause of this discrepancy is in their assumption that the center of the cluster potential coincides with the position of the BCG, while we reveal the BCG position to be  $60''$  outside of the X-ray center.

As shown in this paper, X-ray observations are essential to study gravitational lens phenomena and to determine mass profiles in clusters of galaxies. Hashimoto-dani (1999) found that there is a significant number of samples in which the BCG position deviates from the X-ray peak of the cluster. He suggested that this can be one of the primary causes for the discrepancy in the mass estimates from the X-ray data and from the lensing images.

One advantage of observing low- $z$  gravitational lensing clusters is that it enables us to study X-ray profiles even with an instrument having only moderate spatial resolution. Further detailed studies of the central part of A 3408, such as a temperature gradient and gas distribution within the arc radius, will be enabled with better spatial resolution and larger effective-area instruments, like XMM-Newton. Another advantage is that it becomes possible to examine a lensed image of the source galaxy, if the source redshift is small, as in our case. In fact, we showed that the weak shear of the arc-like object is consistent with the small magnification factor which we derived.

We are grateful to the ASCA team for operating the spacecraft and supporting the data analysis. H.K. is supported by JSPS Research Fellowship for Young Scientists. The computation code for the

lens image and cluster potential used in the last subsection was provided by M. Hattori and M. Murata, Tohoku University.

## References

- Abell, G. O., Corwin, H. G., Jr. & Olowin, R. P. 1989, *ApJS*, 70, 1
- Abramopoulos, F., & Ku, W. H. -M. 1983, *ApJ*, 271, 446
- Allen, S. W. 1998, *MNRAS*, 296, 392
- Allen, S. W., Fabian, A. C., & Kneib, J. P. 1996, *MNRAS*, 279, 615
- Binggeli, B., Sandage, A., & Tammann, G. A. 1988, *ARA&A*, 26, 509
- Blakeslee, J. P., & Metzger, M. R. 1999, *ApJ*, 513, 592
- Campusano, L. E., & Hardy, E. 1996, in *IAU Symp*, 173, *Astrophysical applications of gravitational lensing*, ed. C. S. Kochanek & J. N. Hewitt (Dordrecht: Kluwer), 125
- Campusano, L. E., Kneib, J. -P., & Hardy, E. 1998, *ApJ*, 496, L79
- Dickey, J. M., & Lockman, F. J. 1990, *ARA&A*, 28, 215
- Ebeling, H., Voges, W., Böhringer, H., Edge, A. C., Huchra, J. P., & Briel, U. G. 1996, *MNRAS*, 281, 799
- Faber, S. M., & Jackson, R. E. 1976, *ApJ*, 204, 668
- Gotthelf, E. V., Ueda, Y., Fujimoto, R., Kii, T., & Yamaoka, K. 2000, *ApJ*, 543, 417
- Hashimotodani, K. 1999, Ph. D. Thesis, The University of Osaka
- Hattori, M., Matuzawa, H., Morikawa, K., Kneib, J. -P., Yamashita, K., Watanabe, K., Böhringer, H., & Tsuru, G. T. 1998, *ApJ*, 503, 593
- Ikebe, Y. 1996, Ph. D. Thesis, The University of Tokyo (RIKEN IPCR CR-87)
- Ishisaki, Y. 1996, Ph. D. Thesis, The University of Tokyo (ISAS-RN 613)
- Makino, N., Sasaki, S., & Suto, Y. 1998, *ApJ*, 497, 555
- Makishima, K., Tashiro, M., Ebisawa, K., Ezawa, H., Fukazawa, Y., Gunji, S., Hirayama, M., Idesawa, E. et al. 1996, *PASJ*, 48, 171
- Markevitch, M., Forman, W. R., Sarazin, C. L., & Vikhlinin, A. 1998, *ApJ*, 503, 77
- Navarro, J. F., Frenk, C. S., & White, S. D. M. 1996, *ApJ*, 462, 563

- Ohashi, T., Ebisawa, K., Fukazawa, Y., Hiyoshi, K., Horii, M., Ikebe, Y., Ikeda, H., Inoue, H.  
et al. 1996, PASJ, 48, 157
- Raymond, J. C., & Smith, B. W. 1977, ApJS, 35, 419
- Sarazin, C. L. 1988, "X-ray emissions from clusters of galaxies", (Cambridge: Cambridge University press)
- Tanaka, Y., Inoue, H., & Holt, S. S. 1994, PASJ, 46, L37
- Ueda, Y., Takahashi, T., Inoue, H., Tsuru, T., Sakano, M., Ishisaki, Y., Ogasaka, Y., Makishima, K. et al. 1999, ApJ, 518, 656
- Wu, X. -P., & Fung, L. -Z. 1997, ApJ, 483, 62

Table 1. Spectral fits to the GIS spectra of three regions of A 3408.

Region (kpc)	Temperature (keV)	Abundance (solar)	$\chi^2/\text{d.o.f}$
$r < 250$	$3.0^{+0.3}_{-0.2}$	$0.42^{+0.15}_{-0.21}$	143.0/119
$250 < r < 800$	$2.8^{+0.2}_{-0.3}$	$0.28^{+0.18}_{-0.22}$	252.6/229
$r < 800$	$2.9^{+0.2}_{-0.2}$	$0.34^{+0.20}_{-0.17}$	245.5/238

Table 2. Radial surface-brightness fit to the GIS data with the  $\beta$  model.

$\beta$	$r_c$ ( $h_{50}^{-1}$ kpc)	$S_0$ (count/pix)	background (count/pix)	$\chi^2/\text{d.o.f}$
$0.53 \pm 0.07$	$177 \pm 61$	$6.55 \pm 0.08$	$0.45 \pm 0.01$	41.6/19

Table 3. Radial surface-brightness fit to the GIS data with the NFW model fitting.

$B$	$r_s$ ( $h_{50}^{-1}$ kpc)	$\chi^2/\text{d.o.f}$
$7.7 \pm 1.0$	$632 \pm 204$	43.6/19

### Figure Captions

Fig. 1.  $B + I$  band image of an arc-like object in A 3408 taken with the 0.9 m CTIO telescope (Campusano et al. 1998). The image size is  $2' \times 2'$ . An arc-like object is seen  $50''$  away from the BCG.

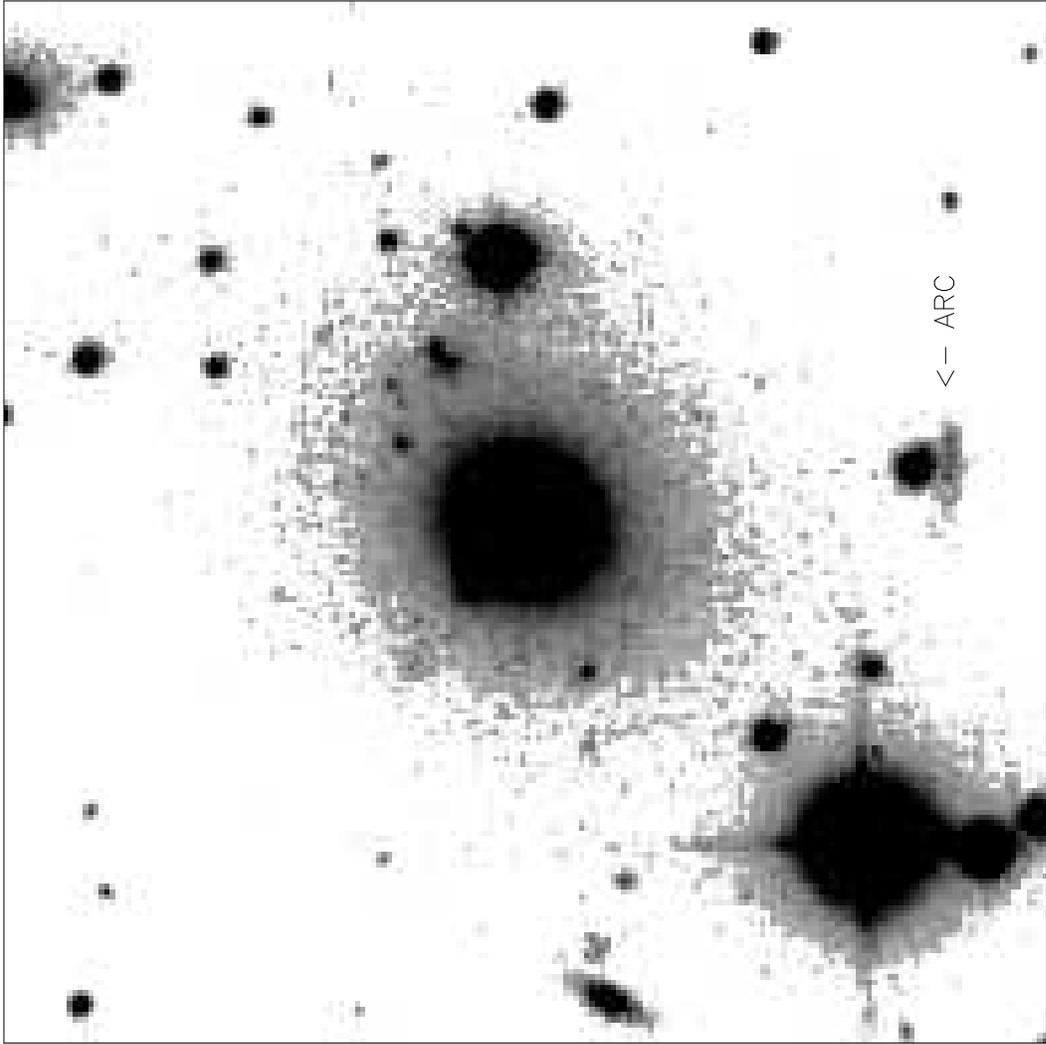
Fig. 2. GIS image of A 3408 (contour) overlaid on an optical image from DSS (Digitalized Sky Survey). The GIS energy range is 0.7–10 keV. The GIS image was smoothed by a  $\sigma = 0.5$  Gaussian filter. The spacing of the contour is linear with a step size of  $4.2 \times 10^{-4}$  count  $s^{-1}$  arcmin $^{-2}$ . The lowest contour is at  $8.6 \times 10^{-4}$  count  $s^{-1}$  arcmin $^{-2}$ . The circle represents the GIS pointing accuracy.

Fig. 3. GIS spectrum of the region  $r < 800$  kpc.

Fig. 4. X-ray surface brightness profile of A 3408. The solid line is the best-fit curve of the  $\beta$ -model fitting and the dotted line is that of the NFW model fitting.

Fig. 5. Projected mass distribution of A 3408.

Fig. 6. Magnifications of a background source at  $z = 0.073$  produced by our lens model of A 3408. The image size is  $100'' \times 100''$ , and the center (0,0) corresponds to the BCG position. The contours indicate magnifications of  $\Delta m = 0.04, 0.05, 0.07, 0.11,$  and  $0.19$  from the outer to the inner. S1 and S2 correspond to the position of the source galaxy derived by Campusano et al. (1998) and by our model, respectively. The cross represents the X-ray peak.



This figure "figure2.gif" is available in "gif" format from:

<http://arxiv.org/ps/astro-ph/0111017v1>

A 3408 ( $r < 800$  kpc)

